Effects of the antiferromagnetic spin structure on antiferromagnetically induced perpendicular magnetic anisotropy

Bo-Yao Wang,[1,*] Ming-Shian Tsai,[1] Chun-Wei Huang,[1] Chun-Wei Shih,[1] Chia-Ju Chen,[1] Kai Lin,[1] Jin-Jhuan Li,[1] Nae-Yeou Jih,[2] Chun-I Lu,[3] Tzu-Hung Chuang,[3] and Der-Hsin Wei[3]

[1]*Department of Physics, National Changhua University of Education, Changhua 500, Taiwan*

[2]*The Center of Teacher Education, National Chung Hsing University, Taichung 402, Taiwan*

[3]*National Synchrotron Radiation Research Center, Hsinchu 300, Taiwan*

(Received 2 July 2017; revised manuscript received 28 August 2017; published 15 September 2017)

Antiferromagnetic (AFM) thin films are promising materials for inducing perpendicular magnetic anisotropy (PMA) in adjacent ferromagnetic (FM) films. This study demonstrates that in a selected AFM spin structure with out-of-plane uncompensated moments, the magnitude of the induced PMA in its neighboring Co/Ni film could be significantly enhanced by the establishment of a collinearlike exchange interaction between the volume moments of the AFM film and the perpendicular magnetic FM film. Detailed magnetic hysteresis loops and x-ray analysis revealed a quench of perpendicular surface anisotropy in a monolayered $Fe_{50}Mn_{50}$/Co/Ni film due to the formation of antiparallel-like coupled Fe and Mn moments. By contrast, the establishment of a three-dimensional quadratic-type AFM spin structure of an $Fe_{50}Mn_{50}$ film triggered parallel-like out-of-plane uncompensated Fe and Mn moments at the interface and reinforced the PMA induced in the Co/Ni film.

DOI: 10.1103/PhysRevB.96.094416

I. INTRODUCTION

Perpendicular magnetic anisotropy (PMA), which characterizes a preferred out-of-plane orientation of spontaneous magnetization in magnetic systems, has attracted considerable research interest in the field of magnetism because of its applicability to current perpendicular magnetological devices [1–4] and close connection to many fundamental magnetic interactions [5–11]. Previous studies have indicated that PMA induced in antiferromagnetic (AFM) thin films is highly sensitive to interactions between magnetic moments occurring at the AFM-ferromagnetic (FM) interface, as well as to those occurring within the AFM layer [5,6,10]. Consequently, for AFM films grown with coherent structures [5], the interplay of the finite-size effect [12] renders the film thickness capable of adjusting the thermal stability of induced PMA. Moreover, the strength of induced PMA is perturbed when the lateral or vertical atomic distance of the AFM film is altered [10]. Recent research has reported that orthogonal interfacial exchange coupling could be another means of enhancing PMA in FM and AFM oxide systems [8,9]. However, investigations of antiferromagnet-induced PMA are restricted to selected systems; thus, the understanding of this phenomenon is limited.

Antiferromagnet-induced PMA was demonstrated in a model system of epitaxially grown expanded-face-centered tetragonal (e-fct) Mn/Co/Ni/Cu(001) magnetic thin films [10]. In this system, the interfacial Mn moments exhibited strong perpendicular crystalline anisotropy, and the magnetic ordering of the volume moments revealed an in-plane layered AFM structure [13,14]. The PMA could have been induced through noncollinear exchange coupling between the interfacial Mn moments and the moments in the volume of the Mn film. However, regarding the e-fct Mn/Co/Ni/Cu(001) films, the strength of the induced PMA was significantly restricted despite the thickening of the Mn film. This observation reveals the limitation of inducing PMA in AFM films with two-dimensional spin structures and indicates that determining the effects of AFM spin structures on induced PMA is essential.

Chemically disordered fcc $Fe_{50}Mn_{50}$ structures have been proposed to exhibit three-dimensional quadratic (3Q) spin ordering with spins pointing along four ⟨111⟩ directions [15–18]. In addition, fcc $Fe_{50}Mn_{50}$ films can engage in strong exchange coupling with perpendicular magnetic films and enhance their magnetic ordering temperature T_{Ordering} through the magnetic proximity effect [15,19,20]. Because fcc $Fe_{50}Mn_{50}$ films can be grown epitaxially on Co(Ni)/Cu(001) films [21], fcc $Fe_{50}Mn_{50}$/Co/Ni/Cu(001) films are considered a suitable alternative to e-fct Mn/Co/Ni/Cu(001) films for examining the effects of the spin structure of AFM films on induced PMA.

The current study explored the effects of an AFM spin structure on antiferromagnet-induced PMA. The study results revealed that fcc $Fe_{50}Mn_{50}$ films could induce PMA on adjacent Co/Ni films after these films had reached a critical thickness associated with the establishment of long-range AFM ordering. A considerably stronger PMA was induced in the fcc $Fe_{50}Mn_{50}$/Co/Ni films than that in the e-fct Mn/Co/Ni films; this was a result of the establishment of a collinearlike exchange interaction between the 3Q AFM spin ordering inside the $Fe_{50}Mn_{50}$ films and perpendicular magnetic FM moments.

II. EXPERIMENT

$Fe_{50}Mn_{50}$/Co/Ni films were prepared on Cu(001) single-crystal substrates and investigated *in situ* in an ultrahigh-vacuum chamber with a base pressure of 2×10^{-10} Torr. The Cu(001) substrates with a 0.1° miscut were cleaned by applying cycles of 2 keV Ar^+ ion sputtering and subsequent annealing at 800 K for 5 min to obtain a well-ordered crystalline structure and smooth morphology [22]. The deposition rate and thickness of the films were monitored by medium-energy electron diffraction (MEED). Figure 1 shows

*bywang1735@cc.ncue.edu.tw

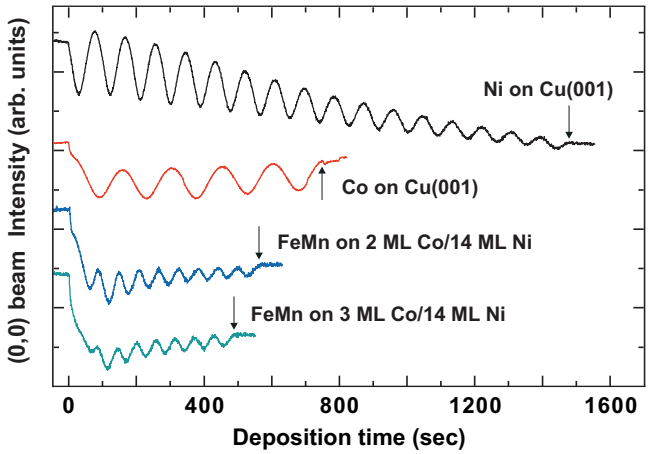

FIG. 1. Selected MEED (0,0) beam intensity curves as a function of deposition time for Ni and Co films grown on Cu(001) and an $Fe_{50}Mn_{50}$ film grown on 2–3-ML Co/14-ML Ni/Cu(001) at 300 K. The thickness of the films was calibrated by the oscillations in the MEED curves. The arrows indicate the time for the shutter to be closed.

the specular MEED (0,0) beam intensity of the Ni and Co films grown on Cu(001) and $Fe_{50}Mn_{50}$ alloy films grown on 2–3-monolayer (ML) Co/14-ML Ni/Cu(001). In both cases, regular oscillation indicates layer-by-layer growth in the films. Preparation of the Co/Ni films on Cu(001) followed the same procedure as that in a previous study [10] to ensure that the films would have the same magnetic properties as those of FM films. The $Fe_{50}Mn_{50}$ alloy films were prepared through the codeposition of the Fe and Mn thermal evaporators. The alloy compositions were calibrated by MEED oscillation.

The average in-plane and vertical interlayer distances of the films were measured by applying low-energy electron diffraction (LEED) with a kinematics approximation (LEED I-V) [23]. The magnetic hysteresis loops of the samples were measured *in situ* in terms of the magneto-optical Kerr effect (MOKE) in longitudinal and polar geometries. The magnetic domain images and x-ray absorption spectra (XAS) of the films were obtained through x-ray photoemission electron microscopy (PEEM) [24–26] by observing x-ray magnetic circular dichroism (XMCD) effects at beamline BL05B2 of the National Synchrotron Radiation Research Center in Hsinchu, Taiwan. The magnetic information of the individual elements was obtained from the asymmetry of the XMCD curves at the corresponding $L_{3,2}$ absorption edges [27]. Contrast normalization was achieved through imaging calculations of two full-field images measured at the Ni, Co, Fe, and Mn L_3 and L_2 edges by applying the formula $(I_{L3} - I_{L2})/(I_{L3} + I_{L2})$ [27], where I_{L3} and I_{L2} are the x-ray absorption intensities of the sample taken at edges L_3 and L_2, respectively. Because of the fully magnetic shielding in the present PEEM end station, the XAS and XMCD spectra measured in total electron yield mode were under remanent condition. The remanent states of the sample were achieved by applying either positive or negative magnetic field along the out-of-plane direction ($\pm$1000 Oe) when it was outside the PEEM. In this study, all measurements were performed at room temperature.

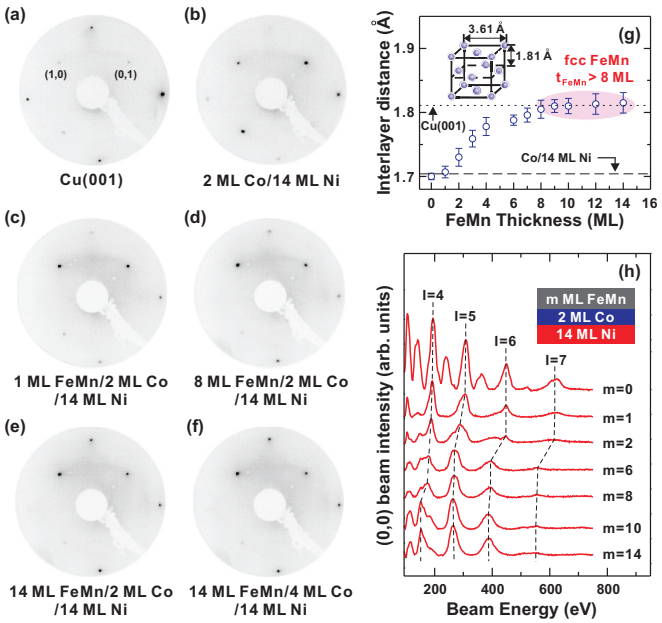

FIG. 2. LEED patterns of (a) Cu(001), (b) 2-ML Co/14-ML Ni/Cu(001), (c) 1-ML $Fe_{50}Mn_{50}$/2-ML Co/14-ML Ni/Cu(001), (d) 8-ML $Fe_{50}Mn_{50}$/2-ML Co/14-ML Ni/Cu(001), (e) 14-ML $Fe_{50}Mn_{50}$/2-ML Co/14-ML Ni/Cu(001), and (f) 14-ML $Fe_{50}Mn_{50}$/4-ML Co/14-ML Ni/Cu(001) films, measured at 110 eV and 300 K. (g) Average $d_\perp$ of various films calculated according to the energy peaks (I) in the I-V curves at room temperature. (h) Selected LEED specular spot I-V curves for various $Fe_{50}Mn_{50}$ films grown on 2-ML Co/14-ML Ni/Cu(001) films measured at 300 K. In (g), the horizontal dotted and dashed lines indicate the $d_\perp$ values of Cu(001) and 2-ML Co/14-ML Ni, respectively, as provided by previous studies [10,28,29].

III. RESULTS

A. Crystalline structures of $Fe_{50}Mn_{50}$/Co/Ni/Cu(001) films

The crystalline structures of $Fe_{50}Mn_{50}$/Co/Ni films grown on Cu(001) were characterized by LEED. Figures 2(a)– 2(f) show selected LEED patterns of Cu(001) and those of the subsequently deposited 2-ML Co/14-ML Ni films and 1–14-ML $Fe_{50}Mn_{50}$ films grown on Co/Ni bilayers at 110 eV. The LEED $P(1 \times 1)$ spots of these films were located at the same positions as those of Cu(001), indicating an epitaxial growth condition. Therefore, the in-plane lattice constants $a_\parallel$ of the $Fe_{50}Mn_{50}$ and Co(Ni) films were equal to the Cu(001) value (approximately 3.61 Å). Because no additional diffraction spots associated with the formation of an ordered alloy were observed, we conclude that the prepared $Fe_{50}Mn_{50}$ layers were chemically disordered crystalline films, a result that is in agreement with those of previous studies [15,20,21].

Figure 2(g) shows the vertical interlayer distance $d_\perp$ of the $Fe_{50}Mn_{50}$ films grown on the Co/Ni bilayers, which was determined according to the corresponding LEED specular spot I-V curves [Fig. 2(h)]. The $d_\perp$ value of the $Fe_{50}Mn_{50}$ films gradually increased from approximately 1.71 to 1.81 Å when the $Fe_{50}Mn_{50}$ film thickness t_{FeMn} was increased from 1 to 8 ML. As the t_{FeMn} level was further increased, the $Fe_{50}Mn_{50}$ films revealed a stable fcc structure, a finding that is consistent with a previous experimental report [21]. However, the $d_\perp$

value of the 2-ML Co/14-ML Ni film was approximately 1.70 Å, which is also consistent with the findings of previous studies [10,28,29].

B. Magnetic properties of $Fe_{50}Mn_{50}$/Co/Ni/Cu(001) films

The magnetic properties of the $Fe_{50}Mn_{50}$/2-ML Co/14-ML Ni films were initially investigated in terms of the MOKE. Figure 3(a) shows the magnetic hysteresis loops of the 0–12-ML $Fe_{50}Mn_{50}$/2-ML Co/14-ML Ni films measured in longitudinal and polar geometries at 300 K. The magnetic anisotropy of the 2-ML Co/14-ML Ni film was aligned in the in-plane direction. PMA was established when the thickness of the covered $Fe_{50}Mn_{50}$ film was greater than 8 ML, a behavior similar to the system of e-fct Mn/2-ML Co/14-ML Ni [Fig. 3(b)], where the induced PMA was observed when the Mn film thickness t_{Mn} was greater than 6 ML. However, the 1-ML Mn/2-ML Co/14-ML Ni film evidently exhibited distinguishable PMA, which was contributed by the perpendicular surface crystalline anisotropy of the monolayer Mn film [6,10]. By contrast, a stable in-plane magnetization was observed in the 1-ML $Fe_{50}Mn_{50}$/2-ML Co/14-ML Ni film.

Figure 4(a) displays the in-plane and out-of-plane remanent magnetizations M_R of the hysteresis loops of various $Fe_{50}Mn_{50}$/2-ML Co/14-ML Ni films. A spin-reorientation transition of the films from the in-plane to the out-of-plane direction occurred when t_{FeMn} was greater than 8 ML. To clarify the correlation between the induced PMA in the $Fe_{50}Mn_{50}$/2-ML Co/14-ML Ni films and the antiferromagnetism of the fcc $Fe_{50}Mn_{50}$ films, it is essential to determine the onset of long-range AFM ordering of the AFM film. In many specimens, x-ray magnetic linear dichroism (XMLD) is a direct approach to examine the AFM order of the AFM film. However, after several tries, our attempts to acquire XMLD spectra similar to those reported by Antel *et al.* [30] were unsuccessful. This might be partly because our experimental setup does not allow us to rotate the sample as Antel *et al.* did. Since the XMLD signal is strong in systems showing the multiplet effect (like NiO or $LaFeO_3$ [31–33]), FeMn is expected to exhibit a weak XMLD signal. Thus, in the present work, we decided to use the enhanced H_C as a fingerprint to indicate the presence of long-range AFM ordering in our samples, as has been justified in previous studies [20,21,27,34–36]. As illustrated in Fig. 4(c), the H_c value was significantly enhanced when t_{FeMn} exceeded 8 ML, indicating a threshold thickness of 8 ML for the established long-range AFM ordering of the $Fe_{50}Mn_{50}$ films. Notably, this threshold thickness is close to the critical $Fe_{50}Mn_{50}$ film thickness associated with the onset of PMA in the $Fe_{50}Mn_{50}$/2-ML Co/14-ML Ni films [Fig. 4(a)]. These results suggest that the PMA observed when the t_{FeMn} value exceeded 8 ML was induced by the AFM $Fe_{50}Mn_{50}$ films through AFM-FM exchange coupling.

Antiferromagnet-induced PMA was observed in the Mn/2-ML Co/14-ML Ni films [Fig. 4(b)]. Notably, the threshold associated with the induced PMA as well as long-range AFM ordering was at $t_{Mn} = 6$–7 ML, a value slightly lower than that of the $Fe_{50}Mn_{50}$ film ($t_{FeMn} = 8$ ML). This result suggests that the e-fct Mn film exhibits a stronger AFM exchange interaction than that of the $Fe_{50}Mn_{50}$ film of identical thickness. Furthermore, fcc-like Mn films have been observed to exhibit a slightly higher AFM ordering temperature than that of FeMn films when the films were in a bulk state

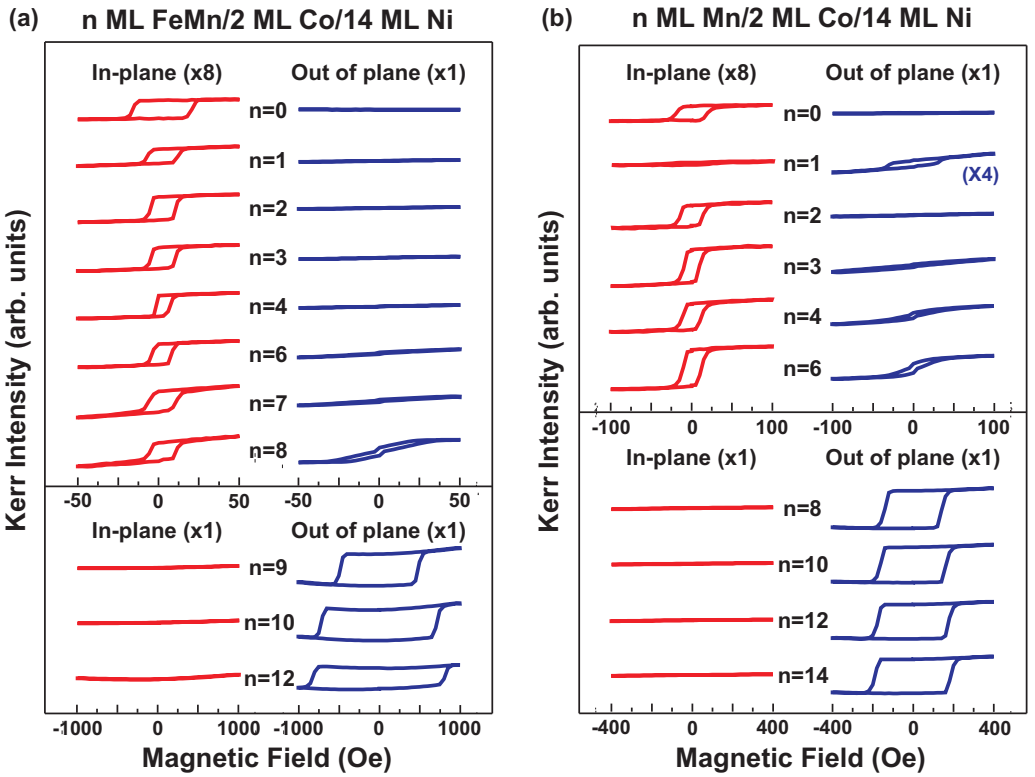

FIG. 3. Magnetic hysteresis loops of (a) 0–12-ML $Fe_{50}Mn_{50}$/2-ML Co/14-ML Ni/Cu(001) and (b) 0–14-ML Mn/2-ML Co/14-ML Ni/Cu(001) films measured according to the longitudinal and polar MOKE at 300 K.

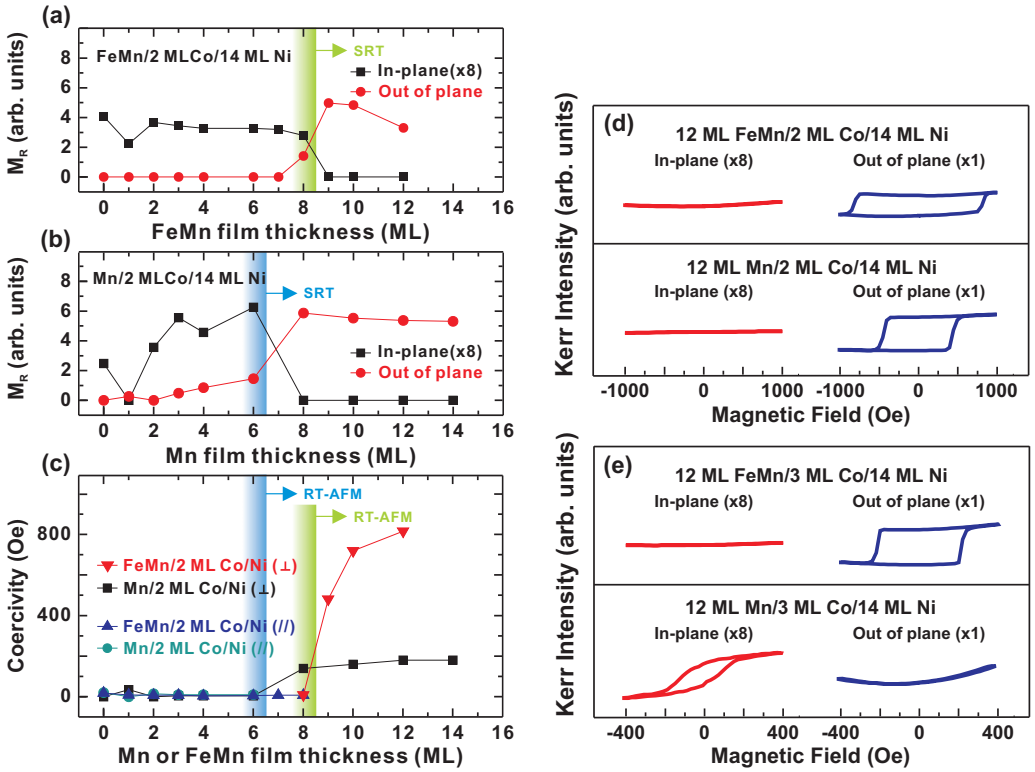

FIG. 4. (a) Remanent magnetization M_R of 0–12-ML $Fe_{50}Mn_{50}$/2-ML Co/14-ML Ni/Cu(001) films. (b) M_R of 0–14-ML Mn/2-ML Co/14-ML Ni/Cu(001) films. (c) Out-of-plane and in-plane coercivity H_C of 0–12-ML $Fe_{50}Mn_{50}$/2-ML Co/14-ML Ni/Cu(001) and 0–14-ML Mn/2-ML Co/14-ML Ni/Cu(001) films. In (c), the arrows indicate the establishment of room-temperature long-range AFM ordering of $Fe_{50}Mn_{50}$ and Mn films. (d) and (e) Magnetic hysteresis loops of 12-ML $Fe_{50}Mn_{50}$ (or Mn)/2-ML Co/14-ML Ni/Cu(001) and 12-ML $Fe_{50}Mn_{50}$ (or Mn)/3-ML Co/14-ML Ni/Cu(001) films, respectively.

(FeMn = 500 K and fcc-like Mn = 540 K) [17,37], and this finding is consistent with those of the present study. However, when the long-range AFM orderings of the fcc $Fe_{50}Mn_{50}$ and e-fct Mn films were well established (i.e., the thickness of the AFM film in each case was above the threshold value), the magnitude of perpendicular H_c induced by the fcc $Fe_{50}Mn_{50}$ films was considerably larger than that induced by the e-fct Mn films. Moreover, as we further enhanced the in-plane magnetic anisotropy of the FM films by increasing the thickness of the Co film from 2 to 3 ML [Figs. 4(d) and 4(e)] [38–40], the 12-ML $Fe_{50}Mn_{50}$ film evidently revealed a higher strength of induced PMA than the 12 ML e-fct Mn film. These results indicate that the volume moments of the fcc $Fe_{50}Mn_{50}$ films could efficiently support the thermal stability of the induced PMA in the Co/Ni film, despite the strength of the AFM exchange interaction possibly being slightly lower than that of the e-fct Mn film.

IV. DISCUSSION

A. Quench of perpendicular surface anisotropy in monolayered FeMn films

Low-dimensional magnetic films can usually engender perpendicular surface anisotropy because of unquenched out-of-plane-oriented orbital moments caused by broken symmetry [5,6,10,41–43]. Based on the results in Fig. 5(a), the 1-ML Mn film or Fe film can induce PMA on the adjacent 2-ML Co/14-ML Ni film. However, this characteristic vanished when the covered layer was replaced by the 1-ML $Fe_{50}Mn_{50}$ film. Investigating the quenching of the perpendicular surface anisotropy when the Fe and Mn elements formed a monolayered AFM alloy film is compelling.

Figures 5(b)– 5(e) show the element-resolved magnetic domain images of the 1-ML $Fe_{50}Mn_{50}$/2-ML Co/14-ML Ni film. Similar domain structure contrast levels could be observed for Ni, Co, and Fe [Figs. 5(b)–5(d)], revealing that their magnetic moments were coupled and aligned in parallel-like orientation in the in-plane direction. By contrast, opposite domain contrast levels could be observed for Mn [Fig. 5(e)], indicating antiparallel-like coupling between the moments of Mn and those of the other three elements.

Applying XMCD sum rules, a previous report on perpendicular magnetic Fe/Ni/Cu(001) has revealed a parallel coupling between the orbital and spin moments of the Fe element, where an orbital value of $0.21\mu_b$–$0.22\mu_b$/atom of the Fe elements was obtained when the thickness of the Fe film decreased from 2 to 0.1 ML [44]. On the other hand, a report on perpendicular magnetic 1-ML Mn/Co/Ni/Cu(001) has shown a high orbital-to-spin ratio of 0.33 for the Mn element, where the direction of orbital moments is also the same as the spin moments [10]. Moreover, previous works on Fe/Mn films (a system of AFM-induced PMA) have also clearly shown a parallel alignment of orbital and spin moments for either the Fe or Mn element, where the interfacial Fe and Mn total moments were found to couple antiparallel along

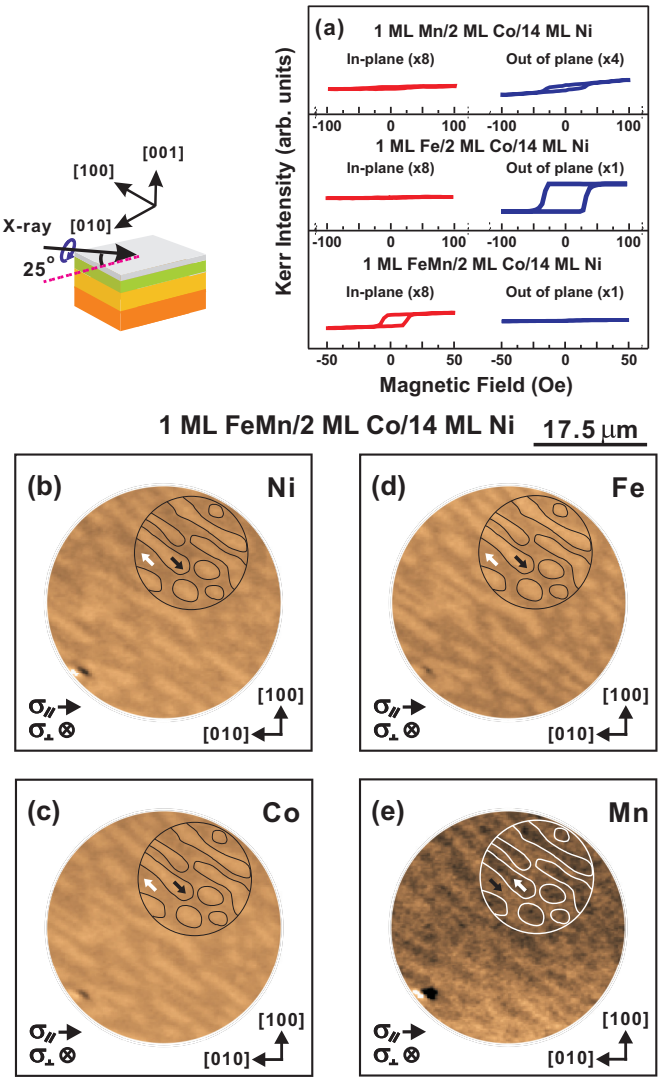

FIG. 5. (a) Magnetic hysteresis loops of 1-ML Mn/2-ML Co/14-ML Ni/Cu(001), 1-ML Fe/2-ML Co/14-ML Ni/Cu(001), and 1-ML $Fe_{50}Mn_{50}$/2-ML Co/14-ML Ni/Cu(001) films. (b) Ni, (c) Co, (d) Fe, and (e) Mn magnetic domain images of a uniform 1-ML $Fe_{50}Mn_{50}$/2-ML Co/14-ML Ni/Cu(001) film measured at 300 K. The top illustration shows that the angle of incident right-circularly polarized (RCP) x-rays was 25° with respect to the in-plane [0$\bar{1}$0] crystallographic direction of Cu(001). In (b)–(e), the black and white arrows displayed on the domain images indicate the magnetization directions of the magnetic moments.

the out-of-plane direction (the out-of-plane orbital moment is approximately $0.46\mu_b$/atom for Mn and $0.14\mu_b$/atom for Fe) [6]. The characteristic that the spin and orbital moments of Fe (or Mn) in FeMn bilayered or alloyed structures coupled in parallel [5,6,10,44–46] could be associated with both elements having filled more than half of their d shells [47–49], where the total angular moments tend to exhibit the largest value according to Hund's rule.

Thus, regarding the 1-ML $Fe_{50}Mn_{50}$/2-ML Co/14-ML Ni film with antiparallel-like coupled Fe and Mn moments in the present study, the overall magnitude of the out-of-plane-oriented orbital moments of the FeMn film, which is considered to be the origin of the perpendicular surface anisotropy, would be reduced relative to that of the film containing a single element. This could hamper the capability of the induced PMA and thus result in in-plane magnetic anisotropy for the 1-ML $Fe_{50}Mn_{50}$/2-ML Co/14-ML Ni film. However, since the two-dimensional quadratic (2Q) spin structure with spins pointing along in-plane ⟨110⟩ directions has been considered the excited state of the FeMn film [18], a contribution of enhanced in-plane-oriented or canted orbital moments of the Fe or Mn element should not be fully excluded.

B. PMA induced by AFM fcc-$Fe_{50}Mn_{50}$ films

In contrast to the behavior of monolayered $Fe_{50}Mn_{50}$, the $Fe_{50}Mn_{50}$ film could induce PMA when $t_{FeMn} > 8$ ML, representing the thickness at which long-range AFM ordering starts to become established [Figs. 3(a) and 6(a)]. According to the XMCD measurements of the 10-ML $Fe_{50}Mn_{50}$/Co/Ni film [Figs. 6(b)–6(d)], the Fe and Mn elements revealed out-of-plane-oriented uncompensated moments that were coupled in parallel-like orientation with the FM moments. Thus, FM ordering of the Fe and Mn uncompensated moments should be deduced. This behavior is expected to be closely linked to an establishment of 3Q-type AFM spin ordering of the $Fe_{50}Mn_{50}$ film because the out-of-plane component of the interfacial Mn and Fe spins in the 3Q structure revealed similar uncompensated features [Figs. 7(a) and 7(c)]. Thus, the formation of a parallel-like alignment between the Fe and Mn interfacial uncompensated moments because of the establishment of long-range AFM ordering of the $Fe_{50}Mn_{50}$ film ensured a constructive superposition of the out-of-plane-oriented orbital moments of the Fe and Mn atoms at the AFM-FM interface; this therefore induced PMA on the adjacent Co/Ni films. This phenomenon is in sharp contrast to the characteristics observed in the monolayered $Fe_{50}Mn_{50}$ film, where the out-of-plane-oriented orbital moments of Fe and Mn were compensated by antiparallel-like coupling (Fig. 5). According to the literature [46,50], AFM FeMn films could possibly cause a reduction in perpendicular magnetization or a twisted magnetic structure on adjacent FM films in FeMn/Ni-based systems due to the formation of a surface step or the competition for the magnetic anisotropy interaction between the interface and volume of the Ni film; however, these complicated effects were possibly considerably weaker in the $Fe_{50}Mn_{50}$/Co/Ni films investigated in the present study because the thickness of the underlying FM films was constantly an integer value and the strength of the induced perpendicular surface anisotropy, which is proportional to the spin-orbital coupling at the interface [5], is much stronger in the $Fe_{50}Mn_{50}$/Co/Ni film.

C. Effects of the AFM spin structure on antiferromagnet-induced PMA

In this section, we discuss why the strength of PMA in the Co/Ni films induced by the $Fe_{50}Mn_{50}$ films was considerably greater than that induced by the e-fct Mn film (Fig. 4). Regarding the behavior of AFM-induced PMA, previous studies have indicated that the thermal stability of induced PMA is supported by the volume moments in AFM

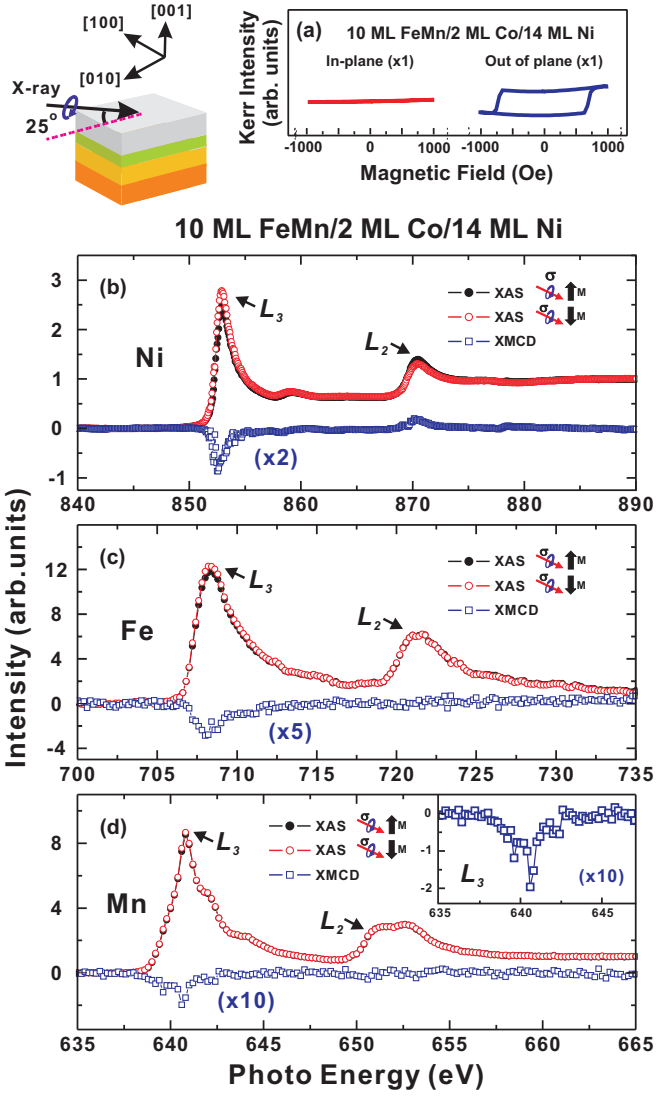

FIG. 6. (a) Magnetic hysteresis loops of 10-ML FeMn/2-ML Co/14-ML Ni/Cu(001) films. X-ray absorption spectrum and corresponding XMCD curves of 10-ML $Fe_{50}Mn_{50}$/2-ML Co/14-ML Ni/Cu(001) measured at the (b) Ni, (c) Fe, and (d) Mn L_3-L_2 edges in the remanent state. The inset in (d) displays the XMCD curve near the Mn L_3 edge. The magnetic fields ($\pm$1000 Oe) were applied to the out-of-plane direction of the sample to achieve two remanent states when it was outside the PEEM end station. The angle of incident RCP x-rays was 25° with respect to the in-plane [0$\bar{1}$0] crystallographic direction of Cu(001).

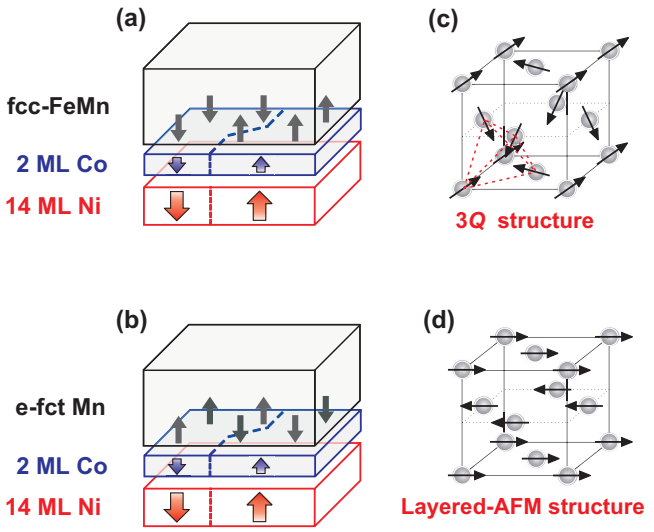

FIG. 7. Illustrations of the interfacial spin structure of (a) fcc $Fe_{50}Mn_{50}$/2-ML Co/14-ML Ni and (b) e-fct Mn/2-ML Co/14-ML Ni films coupled with the FM moments and formed domain structure. The gray arrows displayed in (a) and (b) indicate only the out-of-plane component of the Fe or Mn uncompensated moments. (c) The 3Q and (d) in-plane layered AFM spin structures for the volume moments of the AFM films.

films through a direct exchange interaction [5,6,10]. However, the strength of the exchange interaction transmitted from one magnetic layer to another could strongly depend on the relative spin orientations of the layers. Regarding the $Fe_{50}Mn_{50}$ film with the 3Q-type out-of-plane-oriented uncompensated spin structure [Fig. 7(b)], Lenz *et al.* [20] found that the $Fe_{50}Mn_{50}$ film could engage in strong exchange coupling with the perpendicular magnetic film, significantly enhancing the magnetic ordering temperature in the adjacent FM film through the transmitted exchange interaction (i.e., magnetic proximity effects). The temperature decreased by up to 60 K if the magnetization axis of the FM film was switched from the perpendicular to the in-plane direction. Moreover, considering that a bilayered AFM film was composed of heterospin orderings, Li *et al.* [36] reported that the magnetic ordering temperature of the CoO layer was greatly enhanced by the adjacent NiO layer when the spin orientations of both AFM layers were collinear and aligned in the in-plane direction. By contrast, the magnetic ordering temperature of the CoO layer decreased by approximately 80 K when the spin orientation of the adjacent NiO was switched to the out-of-plane direction, triggered by an increase in the NiO film thickness.

The aforementioned studies have indicated that when the 3Q-type AFM structure of an $Fe_{50}Mn_{50}$ film is well established, the volume moments could couple coherently with the interfacial out-of-plane-oriented Fe and Mn uncompensated moments as well as the adjacent perpendicular magnetic FM film through a collinearlike exchange interaction, thereby efficiently promoting the thermal stability of the induced PMA when t_{FeMn} is increased. By contrast, for the e-fct Mn/Co/Ni films with an in-plane layered AFM spin structure [13,14], the strength of the exchange interaction transmitted from the volume moments of the Mn film [Fig. 7(d)] [6,10] to the perpendicular magnetic interfacial Mn moments and the adjacent perpendicular magnetic FM film could be restricted because of the establishment of a noncollinear-type exchange interaction. Therefore, the strength of induced PMA in the e-fct Mn/Co/Ni films could be limited and insensitive to a further increase in t_{Mn} [Fig. 4(c)]. Although additional theoretical calculations might be necessary to adequately support the proposed physical concept, the present paper provides solid evidence that the spin structure of an AFM film is crucial for the strength of antiferromagnet-induced PMA in AFM-FM bilayers. This finding is essential for the development of the field of antiferromagnet-induced PMA and frontier magnetic

recording technology, which requires perpendicular magnetic films.

V. CONCLUSION

We investigated the effects of an AFM spin structure on antiferromagnet-induced PMA and observed that in a selected AFM spin structure with out-of-plane uncompensated moments, the magnitude of the induced PMA in the neighboring Co/Ni film could be significantly enhanced by the establishment of a collinearlike exchange interaction between the volume moments of the AFM film and perpendicular magnetic FM moments. These findings indicate a method for ameliorating the control of antiferromagnet-induced PMA in AFM-FM heterosystems and could facilitate the development of next-generation perpendicular spintronic devices that exploit the engineering of the AFM spin structures of ultrathin AFM layers.

ACKNOWLEDGMENT

This work was partly supported by the Ministry of Science and Technology, Taiwan (Grant No. MOST 105-2112-M-018-001-MY3).

[1] S. Mangin, D. Ravelosona, J. A. Katine, M. J. Carey, B. D. Terris, and E. E. Fullerton, Nat. Mater. **5**, 210 (2006).
[2] Y. Shiroishi, K. Fukuda, I. Tagawa, H. Iwasaki, S. Takenoiri, H. Tanaka, H. Mutoh, and N. Yoshikawa, IEEE Trans. Magn. **45**, 3816 (2009).
[3] S. Ikeda, K. Miura, H. Yamamoto, K. Mizunuma, H. D. Gan, M. Endo, S. Kanai, J. Hayakawa, F. Matsukura, and H. Ohno, Nat. Mater. **9**, 721 (2010).
[4] D. C. Worledge, G. Hu, D. W. Abraham, J. Z. Sun, P. L. Trouilloud, J. Nowak, S. Brown, M. C. Gaidis, E. J. Ó Sullivan, and R. P. Robertazzi, Appl. Phys. Lett. **98**, 022501 (2011).
[5] B. Y. Wang, N. Y. Jih, W. C. Lin, C. H. Chuang, P. J. Hsu, C. W. Peng, Y. C. Yeh, Y. L. Chan, D. H. Wei, W. C. Chiang, and M. T. Lin, Phys. Rev. B **83**, 104417 (2011).
[6] B.-Y. Wang, J.-Y. Hong, K.-H. O. Yang, Y.-L. Chan, D.-H. Wei, H.-J. Lin, and M.-T. Lin, Phys. Rev. Lett. **110**, 117203 (2013).
[7] B. Y. Wang, C. C. Chiu, W. C. Lin, and M. T. Lin, Appl. Phys. Lett. **103**, 042407 (2013).
[8] P. Kuświk, P. L. Gastelois, M. M. Soares, H. C. N. Tolentino, M. De Santis, A. Y. Ramos, A. D. Lamirand, M. Przybylski, and J. Kirschner, Phys. Rev. B **91**, 134413 (2015).
[9] P. Kuświk, B. Szymański, B. Anastaziak, M. Matczak, M. Urbaniak, A. Ehresmann, and F. Stobiecki, J. Appl. Phys. **119**, 215307 (2016).
[10] B.-Y. Wang, P.-H. Lin, M.-S. Tsai, C.-W. Shih, M.-J. Lee, C.-W. Huang, N.-Y. Jih, P.-Y. Cheng, and D.-H. Wei, Phys. Rev. B **92**, 214435 (2015).
[11] B.-Y. Wang, P.-H. Lin, M.-S. Tsai, C.-W. Shih, M.-J. Lee, C.-W. Huang, N.-Y. Jih, and D.-H. Wei, Phys. Rev. B **94**, 064402 (2016).
[12] T. Ambrose and C. L. Chien, Phys. Rev. Lett. **76**, 1743 (1996).
[13] P.-J. Hsu, Chun-I Lu, Y.-H. Chu, B.-Y. Wang, C.-B. Wu, L.-J. Chen, S.-S. Wong, and M.-T. Lin, Phys. Rev. B **85**, 174434 (2012).
[14] C. B. Wu, J. Song, and W. Kuch, Appl. Phys. Lett. **101**, 012404 (2012).
[15] W. Kuch, L. I. Chelaru, F. Offi, J. Wang, M. Kotsugi, and J. Kirschner, Phys. Rev. Lett. **92**, 017201 (2004).
[16] J. S. Kouvel and J. S. Kasper, J. Phys. Chem. Solids **24**, 529 (1963).
[17] H. Umebayashi and Y. Ishikawa, J. Phys. Soc. Jpn. **21**, 1281 (1966).
[18] M. Ekholm and I. A. Abrikosov, Phys. Rev. B **84**, 104423 (2011).
[19] J. Wang, W. Kuch, L. I. Chelaru, F. Offi, and M. Kotsugi, Appl. Phys. Lett. **86**, 122504 (2005).
[20] K. Lenz, S. Zander, and W. Kuch, Phys. Rev. Lett. **98**, 237201 (2007).
[21] F. Offi, W. Kuch, and J. Kirschner, Phys. Rev. B **66**, 064419 (2002).
[22] M. T. Lin, W. C. Lin, C. C. Kuo, and C. L. Chiu, Phys. Rev. B **62**, 14268 (2000).
[23] W. C. Lin, C. C. Kuo, C. L. Chiu, and M. T. Lin, Surf. Sci. **478**, 9 (2001).
[24] J. Stöhr, Y. Wu, B. D. Hermsmeier, M. G. Samant, G. R. Harp, S. Koranda, D. Dunham, and B. P. Tonner, Science **259**, 658 (1993).
[25] C. M. Schneider and G. Schönhense, Rep. Prog. Phys. **65**, 1785 (2002).
[26] D.-H. Wei, Y.-L. Chan, and Y.-J. Hsu, J. Electron Spectrosc. Relat. Phenom. **185**, 429 (2012).
[27] J. Stöhr and H. C. Siegmann, *Magnetism: From fundamentals to Nanoscale Dynamics* (Springer, Berlin, 2006).
[28] M. Zheng, J. Shen, P. Ohresser, Ch. V. Mohan, M. Klaua, J. Barthel, and J. Kirschner, J. Appl. Phys. **85**, 5060 (1999).
[29] W. Platow, U. Bovensiepen, P. Poulopoulos, M. Farle, K. Baberschke, L. Hammer, S. Walter, S. Müller, and K. Heinz, Phys. Rev. B **59**, 12641 (1999).
[30] W. J. Antel, Jr., F. Perjeru, and G. R. Harp, Phys. Rev. Lett. **83**, 1439 (1999).
[31] A. Scholl, J. Stöhr, J. Lüning, J. W. Seo, J. Fompeyrine, H. Siegwart, J. P. Locquet, F. Nolting, S. Anders, E. E. Fullerton, M. R. Scheinfein, and H. A. Padmore, Science **287**, 1014 (2000).
[32] F. Nolting, A. Scholl, J. Stöhr, J. W. Seo, J. Fompeyrine, H. Siegwart, J. P. Locquet, S. Anders, J. Lüning, E. E. Fullerton, M. F. Toney, M. R. Scheinfein, and H. A. Padmore, Nature (London) **405**, 767 (2000).
[33] H. Ohldag, A. Scholl, F. Nolting, S. Anders, F. U. Hillebrecht, and J. Stöhr, Phys. Rev. Lett. **86**, 2878 (2001).
[34] J. Nogués and I. K. Schuller, J. Magn. Magn. Mater. **192**, 203 (1999).
[35] C. Won, Y. Z. Wu, H. W. Zhao, A. Scholl, A. Doran, W. Kim, T. L. Owens, X. F. Jin, and Z. Q. Qiu, Phys. Rev. B **71**, 024406 (2005).
[36] Q. Li, J.-H. Liang, Y.-M. Luo, Z. Ding, T. Gu, Z. Hu, C.-Y. Hua, H.-J. Lin, T.-W. Pi, S.-P. Kang, C. Won, and Y.-Z. Wu, Sci. Rep. **6**, 22355 (2016).
[37] Y. Endoh and Y. Ishikawa, J. Phys. Soc. Jpn. **30**, 1614 (1971).
[38] B. Schulz and K. Baberschke, Phys. Rev. B **50**, 13467 (1994).

[39] J. Hong, R. Q. Wu, J. Lindner, E. Kosubek, and K. Baberschke, Phys. Rev. Lett. **92**, 147202 (2004).
[40] T. Burkert, O. Eriksson, P. James, S. I. Simak, B. Johansson, and L. Nordström, Phys. Rev. B **69**, 104426 (2004).
[41] D. Peterka, A. Enders, G. Haas, and K. Kern, Phys. Rev. B **66**, 104411 (2002).
[42] B. Heinrich, Z. Celinski, J. F. Cochran, A. S. Arrott, and K. Myrtle, J. Appl. Phys. **70**, 5769 (1991).
[43] U. Gradmann, in *Handbook of Magnetic Materials*, edited by K. H. J. Buschow (North-Holland, Amsterdam, 1993), Vol. 7, Chap. 1, pp. 1–96.
[44] H. Abe, K. Amemiya, D. Matsumura, S. Kitagawa, H. Watanabe, T. Yokoyama, and T. Ohta, J. Magn. Magn. Mater. **302**, 86 (2006).
[45] D. Schmitz, E. Schierle, N. Darowski, H. Maletta, E. Weschke, and M. Gruyters, Phys. Rev. B **81**, 224422 (2010).
[46] K. Amemiya, M. Sakamaki, M. Mizusawa, and M. Takeda, Phys. Rev. B **89**, 054404 (2014).
[47] J. Dresselhaus, D. Spanke, F. U. Hillebrecht, E. Kisker, G. van der Laan, J. B. Goedkoop, and N. B. Brookes, Phys. Rev. B **56**, 5461 (1997).
[48] R. Wu, D. Wang, and A. J. Freeman, Phys. Rev. Lett. **71**, 3581 (1993).
[49] The three-dimensional electron occupation numbers of the Fe and Mn elements are 6.61 and 5.23, respectively [47,48].
[50] J. Wu, J. Choi, A. Scholl, A. Doran, E. Arenholz, C. Hwang, and Z. Q. Qiu, Phys. Rev. B **79**, 212411 (2009).